SUPPLEMENTARY DATA

Structures of proline-rich peptides bound to the ribosome reveal a common mechanism of protein synthesis inhibition

Matthieu G. Gagnon[1,3,*], Raktim N. Roy[2,3], Ivan B. Lomakin[1], Tanja Florin[4], Alexander S. Mankin[4] and Thomas A. Steitz[1,2,3,*]

[1] Department of Molecular Biophysics and Biochemistry, Yale University, New Haven, CT 06520-8114, USA

[2] Department of Chemistry, Yale University, New Haven, CT 06520-8107, USA

[3] Howard Hughes Medical Institute, Yale University, New Haven, CT 06520-8114, USA

[4] Center for Pharmaceutical Biotechnology, University of Illinois at Chicago, Chicago, IL 60607-7173, USA

[*] To whom correspondence should be addressed. Tel: 1-203-432-5619; Fax: 1-203-432-3282; Email: thomas.steitz@yale.edu

Correspondence may also be addressed to Matthieu G. Gagnon. Tel: 1-203-432-5795; Fax: 1-203-432-3282; Email: matthieu.gagnon@yale.edu

The authors wish it to be known that, in their opinion, the first two authors should be regarded as joint First Authors.

This file contains five supplementary figures and one supplementary table.

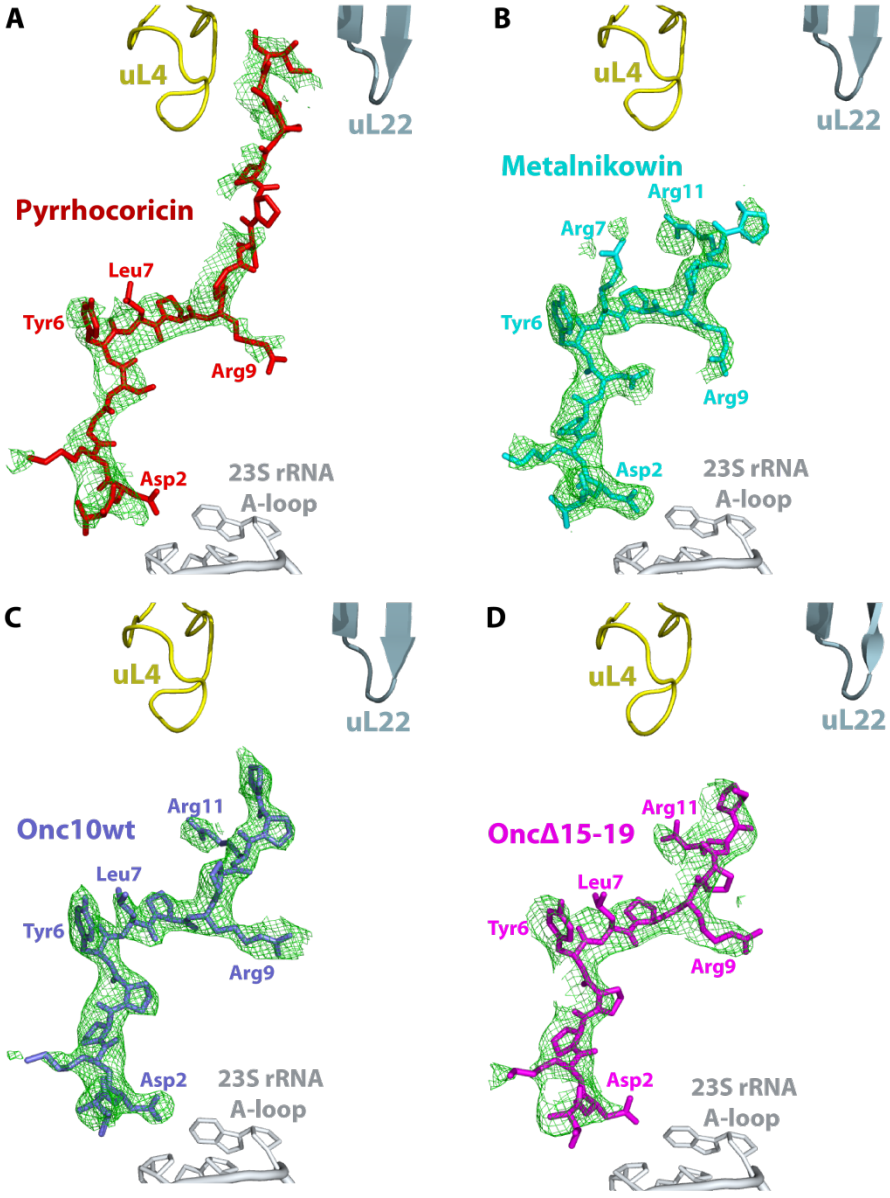

Supplementary Figure S1. Structures of Pyrrhocoricin **(A)**, Metalnikowin **(B)**, Onc10wt **(C)** and OncΔ15-19 **(D)** bound inside the peptide exit tunnel of the ribosome with their difference Fourier $F_{obs} - F_{calc}$ (green) electron density maps shown and contoured at ~2.5σ. The 23S rRNA A-loop and ribosomal proteins uL4 and uL22 are shown. Each peptide is colored as in the main figure 2.

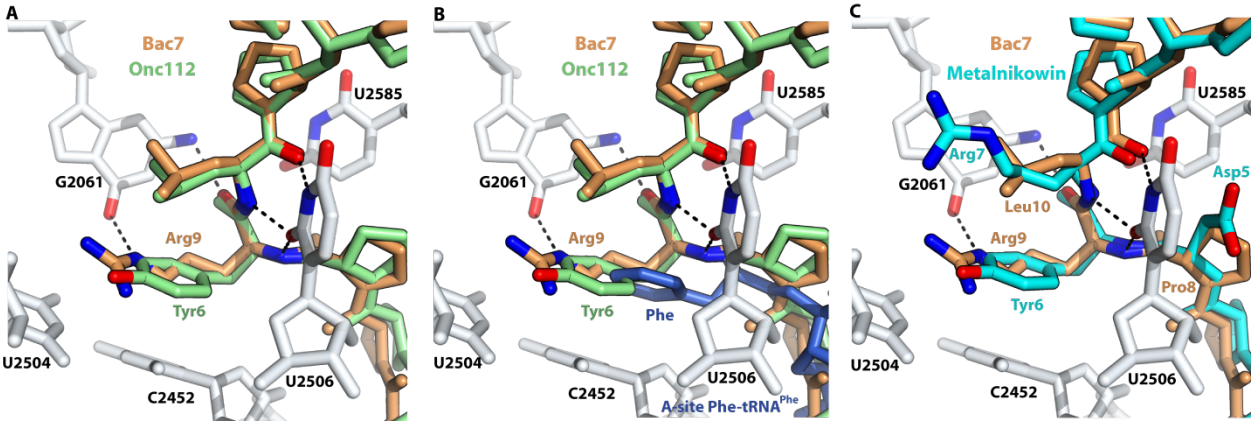

Supplementary Figure S2. Interactions of different PrAMPs with the A-site cleft of the peptide exit tunnel. **(A)** Residue Arg9 in $Bac7_{1\text{-}35}$ overlaps with residue Tyr6 in Onc112 [PDB 4Z8C (1)], thereby forming a similar π-stacking interaction with nucleotide C2452. **(B)** The phenylalanine residue attached to the A-site tRNA occupies the same position in the A-site cleft [PDB 1VY4 (2)]. **(C)** Even though the amino acid sequence of peptide Metalnikowin is slightly different, its Arg7 residue stacks with the previous residue similarly as in the $Bac7_{1\text{-}35}$ peptide.

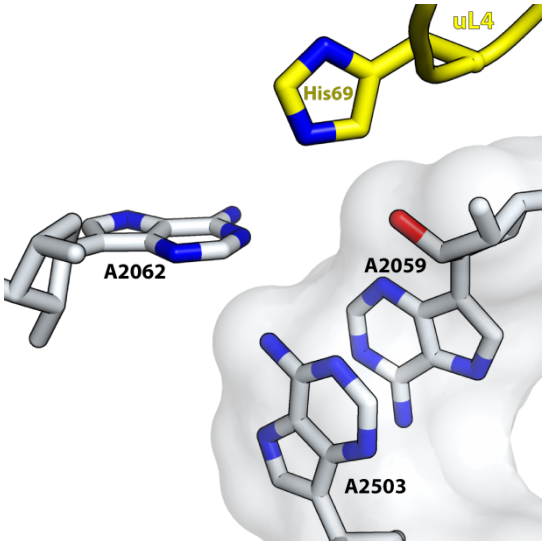

Supplementary Figure S3. Surroundings of nucleotide A2062 in the upper chamber of the peptide exit tunnel. Alterations at 23S rRNA residues A2503 and A2059, which interact with A2062, are expected to affect the position of A2062.

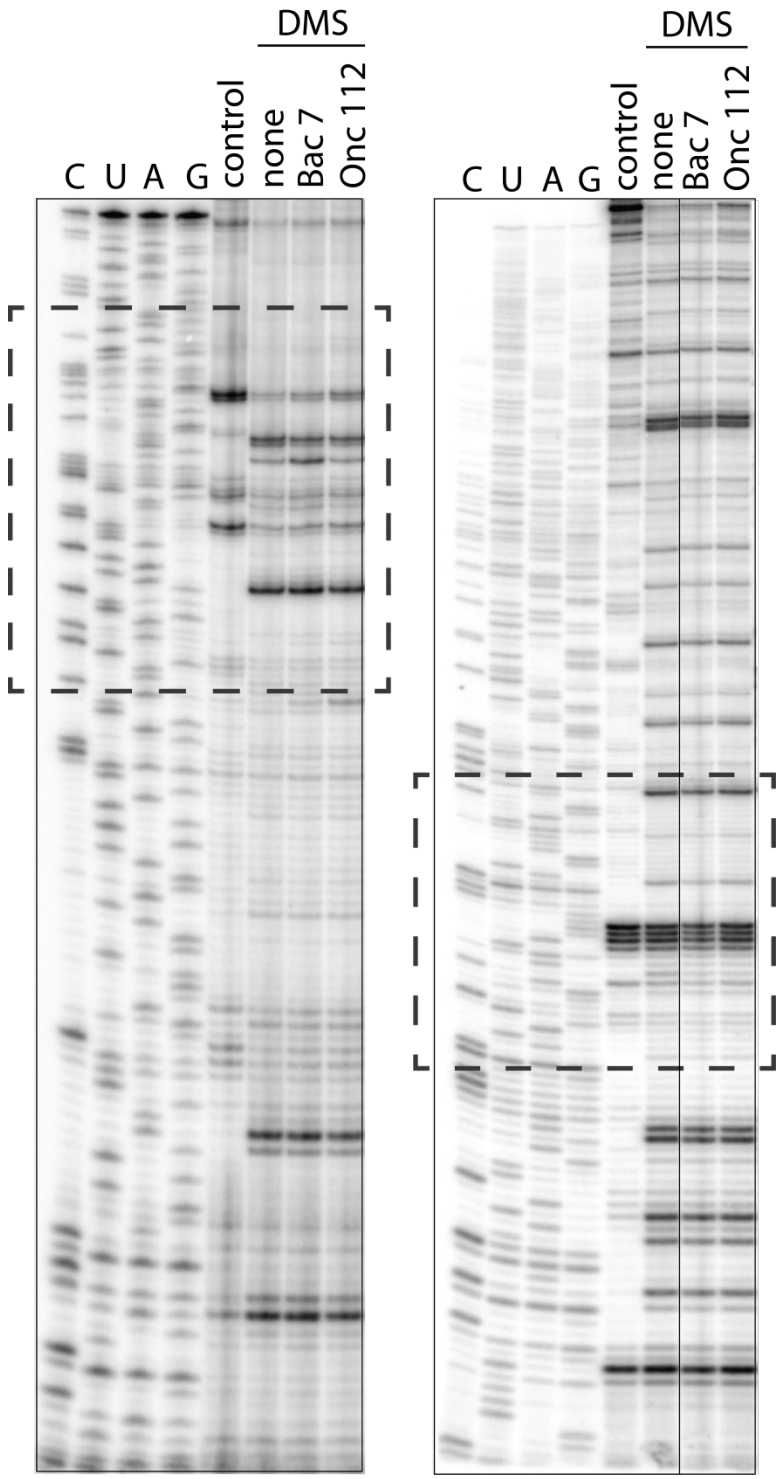

Supplementary Figure S4. The results of $Bac7_{1-35}$ and Onc112 foot-printing on the *E. coli* ribosome. Shown are the full gels, with the gel segments shown in the main figure 1 indicated by the dashed rectangles.

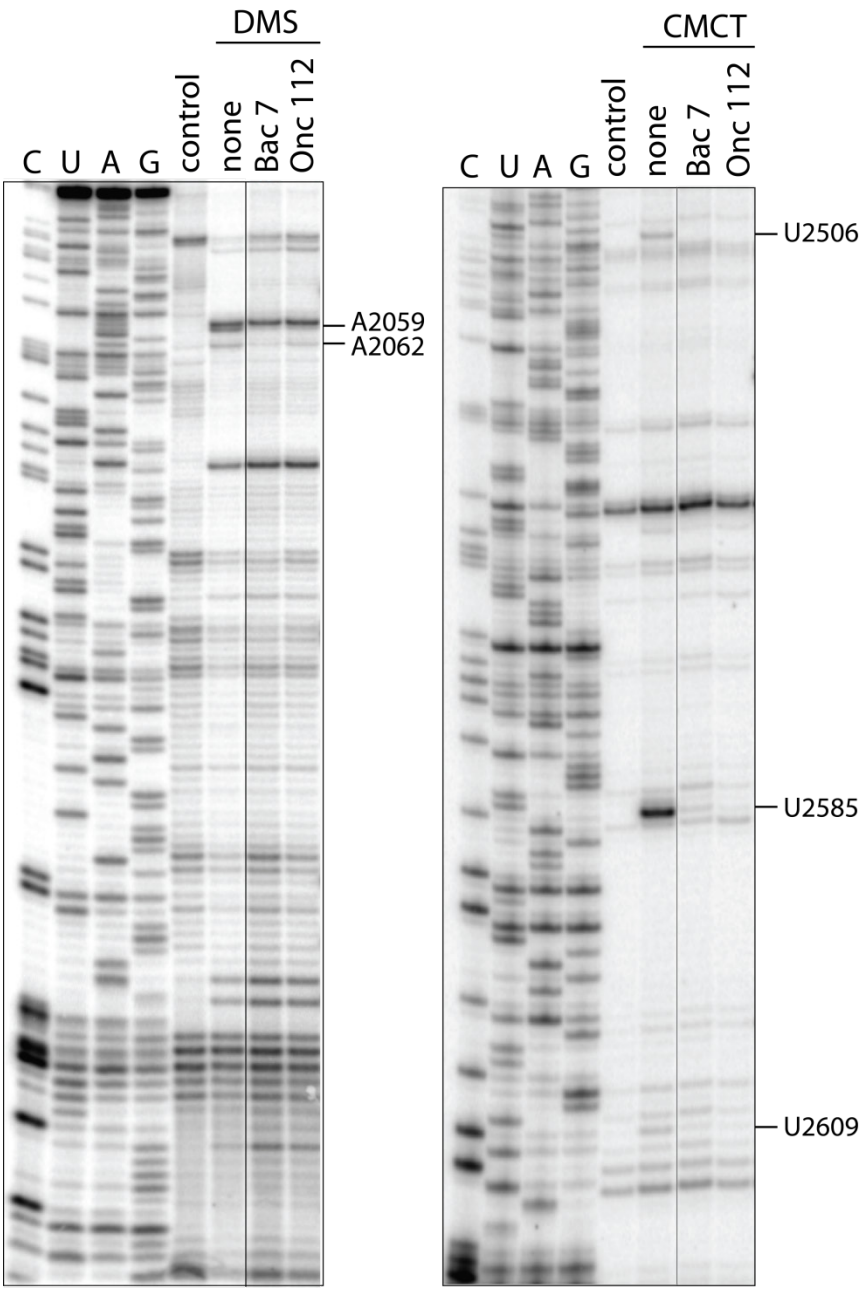

Supplementary Figure S5. Foot-printing of $Bac7_{1-35}$ and Onc112 on the *T. thermophilus* ribosome. The 70S ribosome was pre-incubated with no PrAMP ('none') or 50 μM of $Bac7_{1-35}$ or Onc112 and subjected to modification by DMS or CMCT. The rRNA residues whose accessibility to the modifying reagents was affected by PrAMPs are marked.

Supplementary Table S1. Data collection and refinement statistics.

	70S:L9$_{58}$-Bac7$_{1-35}$ (with EF-G)	70S-Metalnikowin	70S-Onc10wt	70S-OncΔ15-19	70S-Pyrrhocoricin
Data collection					
Space group	$P2_12_12_1$	$P2_12_12_1$	$P2_12_12_1$	$P2_12_12_1$	$P2_12_12_1$
Cell dimensions					
a, *b*, *c* (Å)	208.78, 449.03, 619.34	209.87, 450.49, 623.11	209.83, 450.81, 622.72	210.05, 450.75, 623.36	210.01, 450.13, 622.84
α, β, γ (°)	90.0, 90.0, 90.0	90.0, 90.0, 90.0	90.0, 90.0, 90.0	90.0, 90.0, 90.0	90.0, 90.0, 90.0
Resolution (Å)	50 – 3.0 (3.18 – 3.0)	50 – 2.89 (3.07 – 2.89)	50 – 2.80 (2.97 – 2.80)	50 – 2.80 (2.97 – 2.80)	50 – 2.70 (2.86 – 2.70)
R_{merge} (%)	26.3 (119.8)	21.6 (124.1)	22.1 (164.5)	16.1 (139.5)	16.3 (134.0)
$I / \sigma I$	7.04 (1.34)[a]	9.07 (1.24)[b]	7.79 (1.01)[c]	10.8 (1.29)[d]	9.54 (1.12)[e]
Completeness (%)	99.1 (98.1)	98.6 (94.7)	99.0 (97.8)	99.6 (98.9)	99.3 (98.2)
No. of reflections					
Observed	5,295,862	6,250,510	7,075,688	7,162,802	7,843,380
Unique	1,140,965	1,277,977	1,417,926	1,426,619	1,584,056
Redundancy	4.642 (4.488)	4.891 (4.588)	4.990 (4.903)	5.021 (5.032)	4.951 (4.952)
Refinement					
R_{work} / R_{free} (%)	20.56 / 26.02	21.26 / 26.78	21.52 / 26.87	20.01 / 25.04	22.02 / 27.31
No. of atoms					
Protein	105,244	90,538	90,530	90,523	90,573
RNA	196,511	191,321	191,321	191,321	191,321
Ion	1957	2508	2450	2458	2629
Water	2461	4445	4209	4052	4088
B factors					
Protein	65.1	63.7	62.4	64.0	62.0
RNA	56.7	58.9	58.0	58.8	57.2
Ion	44.6	51.7	51.0	55.3	50.9
Water	40.5	44.1	42.9	46.6	40.4
r.m.s. deviations					
Bond lengths (Å)	0.005	0.006	0.006	0.008	0.006
Bond angles (°)	0.981	0.979	0.999	1.218	0.986

Values in parentheses are for the highest-resolution shell.

[a] I/σI = 2 at ~3.1 Å resolution

[b] I/σI = 2 at ~3.0 Å resolution

[c] I/σI = 2 at ~3.0 Å resolution

[d] I/σI = 2 at ~2.9 Å resolution

[e] I/σI = 2 at ~2.85 Å resolution

Supplementary References

1. Roy, R.N., Lomakin, I.B., Gagnon, M.G. and Steitz, T.A. (2015) The mechanism of inhibition of protein synthesis by the proline-rich peptide oncocin. *Nat. Struct. Mol. Biol.*, **22**, 466-469.
2. Polikanov, Y.S., Steitz, T.A. and Innis, C.A. (2014) A proton wire to couple aminoacyl-tRNA accommodation and peptide-bond formation on the ribosome. *Nat. Struct. Mol. Biol.*, **21**, 787-793.